HENRY GRANJON PRIZE COMPETITION 2006 Co-Winner, Category A "Joining and fabrication technology"

NUMERICAL MODELLING OF HEAT TRANSFER, FLUID FLOW AND MICROSTRUCTURAL EVOLUTION DURING FUSION WELDING OF ALLOYS[1]

W. Zhang

Department of Materials Science and Engineering, The Pennsylvania State University (United States)

ABSTRACT

The present study focuses on modelling numerous aspects of the welding process which include predictions of molten metal convection in the weld pool, size and shape of the fusion zone (FZ) and heat-affected zone (HAZ), temperature distributions in the FZ and HAZ, solidification conditions of the FZ, and phase transformation kinetics in the HAZ. Integrated models were developed taking into account the interactions of heat, fluid flow and microstructure. In particular, a three-dimensional heat transfer and fluid flow model was used to understand the weld pool phenomena and provided useful insight into the physics of the weld pool. Application of the computed thermal cycles and phase transformation models including Johnson-Mehl-Avrami equation and Monte Carlo simulation provided useful tools to understand the microstructural evolution during welding. The developed models were used to investigate several welding processes such as gas metal arc welding (GMAW) and gas tungsten welding (GTAW) and different materials including AISI 1005 low carbon steel, 1045 mild carbon steel, Ti-6Al-4V alloy and 2025 duplex stainless steel. This paper is an extensive summary of the doctoral research work carried out by the author at the Pennsylvania State University.

IIW-Thesaurus keywords: *Simulating; Heat flow; Microstructure; Prediction; Fusion welding; Fusion zone; Weld zone; Heat affected zone; GMA welding; Arc welding; Gas shielded arc welding; GTA welding; Temperature distribution; Solidification; Transformation; Thermal cycling; Practical investigations; Comparisons; Low carbon steels; Steels; Unalloyed steels; Duplex stainless steels; Stainless steels; Titanium alloys; Reference lists.*

1 GENERAL BACKGROUND

Welding expenditures represent a substantial contribution to world economy. The welding technology has been used extensively in the energy, shipbuilding, automotive, aircraft, aerospace and many other industries. Understanding the welding processes and improving the safety and reliability of the welded joints have been an important goal in the welding research. It has been well recognized that the welding process is extremely complex involving arc and plasma physics, high-temperature chemistry, transport phenomena, thermodynamics, metallurgy, mechanics and other disciplines [1, 2].

Doc. IIW-1748-06 (ex-doc. XII-1890-06) recommended for publication by Commission XII "Arc welding processes and production systems".

[1] This research work was supervised by Prof. Tarasankar DebRoy of the Pennsylvania State University, University Park, Pennsylvania, USA, and Dr. John W. Elmer of Lawrence Livermore National Laboratory, Livermore, California, USA.

In fusion welding, the interaction between the base material and the heat source leads to a series of physical and chemical processes [1, 2]. In the weld pool, the molten material undergoes strong circulation, which is driven by the buoyancy, surface tension gradient, gas jet impingement, and, when electric arc is used, electromagnetic forces. Depending on the shielding gas used, partitioning of nitrogen, oxygen and hydrogen into the molten pool may take place. In the solid region around the weld pool, the variation of temperature with time, often referred to as the thermal cycle, may lead to various solid-state phase transformations and changes in the grain structure. These physical and chemical processes affect the composition, geometry, structure and properties of the welded joints. Since a welding process typically involves a large number of variables, studies based on experiments with adequate number of databases are expensive and time consuming, if not impractical. A practical recourse is to simulate the welding process by solving a set of equations representing the essential physical processes of welding.

Numerical modelling of the complex welding process has been traditionally divided into a number of simple constituent parts which include heat transfer, fluid flow, microstructure evolution, and stresses and distortion predictions. In the last few decades, modelling of these constituent parts has evolved greatly. Though significant progress has been made in understanding the individual components, integrated weld modelling, which combines the knowledge of the constituent parts, is still evolving. For example, the temperature distribution (i.e., thermal cycles) is a prerequisite for understanding the microstructure and residual stresses of the weldment. The thermal cycles are often obtained by heat transfer analyses which neglect the melt flow in the weld pool. The calculated thermal cycles may be inaccurate or extensive calibrations may be needed in order to obtain reliable results. Furthermore, the prediction of microstructure or residual stress might be erroneous due to the inaccuracy of the calculated thermal cycles. Comprehensive heat transfer and fluid flow analysis based on weld pool transport phenomena can be used successfully to predict weld bead geometry and temperature distribution. However, the integration of the knowledge obtained in the thermal-fluid model with the microstructure and mechanical models is still evolving.

The goal of the present research work is to develop a methodology, which synthesizes knowledge from various disciplines and embodies the advanced numerical tools and welding experiments, and to apply it to understand various welding processes and welded materials. The present research focuses particularly on the development and application of the thermal-fluid-microstructure models.

This paper serves as an extensive summary of the doctoral research work carried out by the author at the Pennsylvania State University. The details of the research work are available in the literature [3-12].

2 SCOPE OF RESEARCH AND METHODOLOGY

This study focuses on modelling numerous aspects of the welding process which include predictions of molten metal convection in the weld pool, size and shape of the fusion zone (FZ) and heat-affected zone (HAZ), temperature distributions in the FZ and HAZ, solidification conditions of the FZ, and phase transformation kinetics in the HAZ. To achieve these objectives, comprehensive numerical models were developed, and the models were validated by comparing the computed results with the experimental data. The methodology used in the present research is depicted in Figure 1. As shown in this figure, a three-dimensional heat transfer and fluid flow model considering complex joint geometry was developed to calculate the weld bead geometry, temperature and velocity fields in the weld pool, and the thermal cycles in the entire weldment. The phase transformation kinetics was then simulated by coupling the phase transformation models with the computed temperature history information in the weldment. A recently developed x-ray diffraction technique was used to obtain the phase transformation data on real-time under welding conditions [8, 10]. The unique kinetic data obtained using the

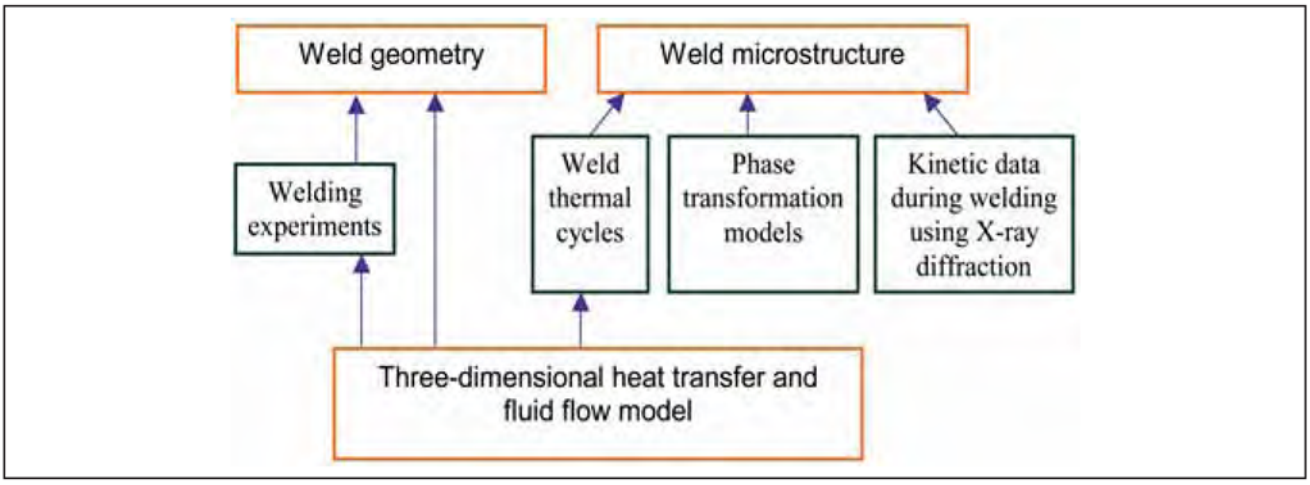

Figure 1 – Research methodology used in the present study

x-ray diffraction technique was then used in the phase transformation models to understand the weld microstructure.

To check the capabilities of the research methodology and the developed models, several welding processes and different materials were investigated. Figure 2 summarizes the various cases studies and their relationship. For the heat transfer and fluid flow modelling, the welding processes studied included gas tungsten arc (GTA) linear [4], GTA spot [5] and gas metal arc (GMA) welding [6, 7]. The temperature distribution in the weldment attains quasi-steady state during GTA linear welding, whereas it varies with time during spot welding. The GMA fillet welding is characterized by complex joint geometry containing a deformable weld pool free surface to account for filler metal additions. The calculated weldment geometry was validated against the experimental data under various welding conditions. For the modelling of microstructural evolution, the welded materials investigated included AISI 1005 low carbon steel [8, 9], 1045 mild carbon steel [10], 2205 duplex stainless steel (DSS) [11] and Ti-6Al-4V alloy [12]. The calculated phase transformation kinetics were compared with those obtained using the spatially and time resolved x-ray diffraction techniques.

It should be noted that the case studies shown in Figure 2 follow an approach of moving from simple to complex systems. For example, among the three welding processes, the GTA linear welding is the simplest one since the system of interest is at steady state, whereas the GMA welding is the most complicated one in that it involves free surface flow and complex joint geometry. Similarly, the microstructure in the carbon steel weldment has been widely studied, but not so in the duplex stainless steel and Ti-based alloy. Such method ensures that the models developed here can be effectively adapted to understand more complex welding processes and new materials.

3 SIGNIFICANT FINDINGS OF RESEARCH

The numerical models used in the present research work included the following.

(1) An existing transient heat transfer and fluid flow model was utilized for the calculation of the evolution of temperature and velocity fields during arc spot welding [5].

(2) A three-dimensional heat transfer and free surface flow model was developed for GMA fillet welding considering the complex weld joint geometry [6, 7].

(3) A kinetic model based on the Johnson-Mehl-Avrami (JMA) theory was developed for the calculation of phase transformation kinetics [4, 8-10].

(4) An existing Monte Carlo model was used to simulate the grain growth [9].

(5) An austenite decomposition model was used to compute the weld final microstructure [4, 9].

(6) A one-dimensional numerical diffusion model considering multiple moving interfaces was developed to understand phase transformation kinetics in a duplex stainless steel [11].

As shown in Figure 2, the integrated numerical models together with advanced welding experiments were applied to study the heat transfer, fluid flow and microstructural evolution during fusion welding of several important engineering alloys. Some of the significant research findings are summarized as follows.

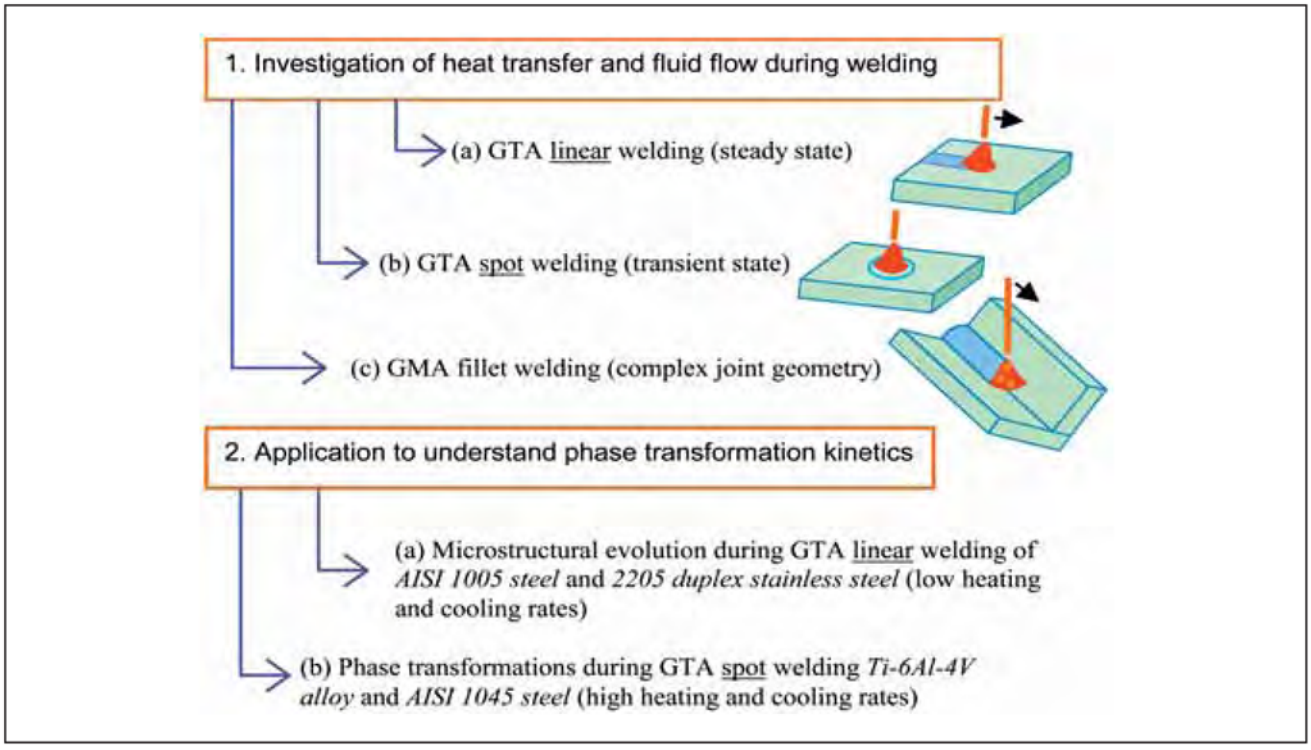

Figure 2 – Various cases investigated in the present research and their relationship

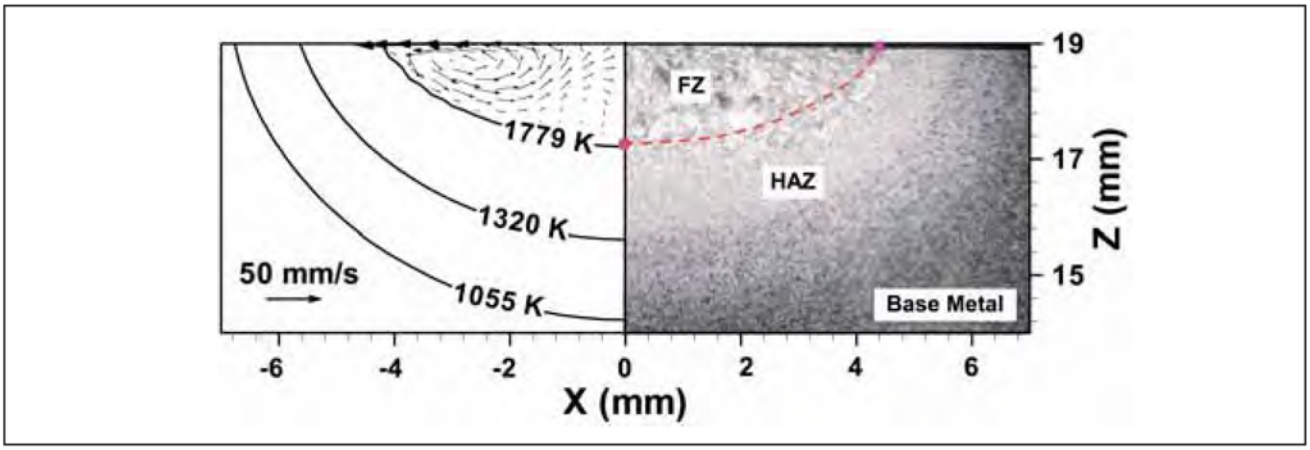

Figure 3 – Calculated and measured weld pool geometry during GTA spot welding

3.1 Heat transfer and fluid flow during transient spot welding

The evolution of temperature and velocity fields during GTA spot welding of AISI 1005 steel was studied using a transient numerical model [5]. The calculated geometry of the weld FZ and HAZ and the weld thermal cycles were in good agreement with the corresponding experimental results, as shown in Figures 3 and 4, respectively. During solidification, the mushy zone grew significantly with time until the pure liquid region vanished. The solidification rate (R) of the mushy zone/solid interface was shown to increase, while the temperature gradient (G) in the mushy zone at this interface was shown to decrease as solidification of the weld pool progressed. As shown in Figure 5, tracking the solidification parameter G/R with time shows that the weld pool solidified with decreasing interface stability, i.e., with a higher tendency to form dendrites towards the centre of the weld. The computed cooling rates and solidification velocities are useful data for determining the solidification morphology and the scale of the solidification substructure.

3.2 Heat transfer and free surface flow in complex weld joints

GMA fillet welding is one of the most important processes for metal joining in shipbuilding and other heavy manufacturing industries because of its high productivity and amiability to automation. Performance of structurally sound fillet welds is largely determined by the

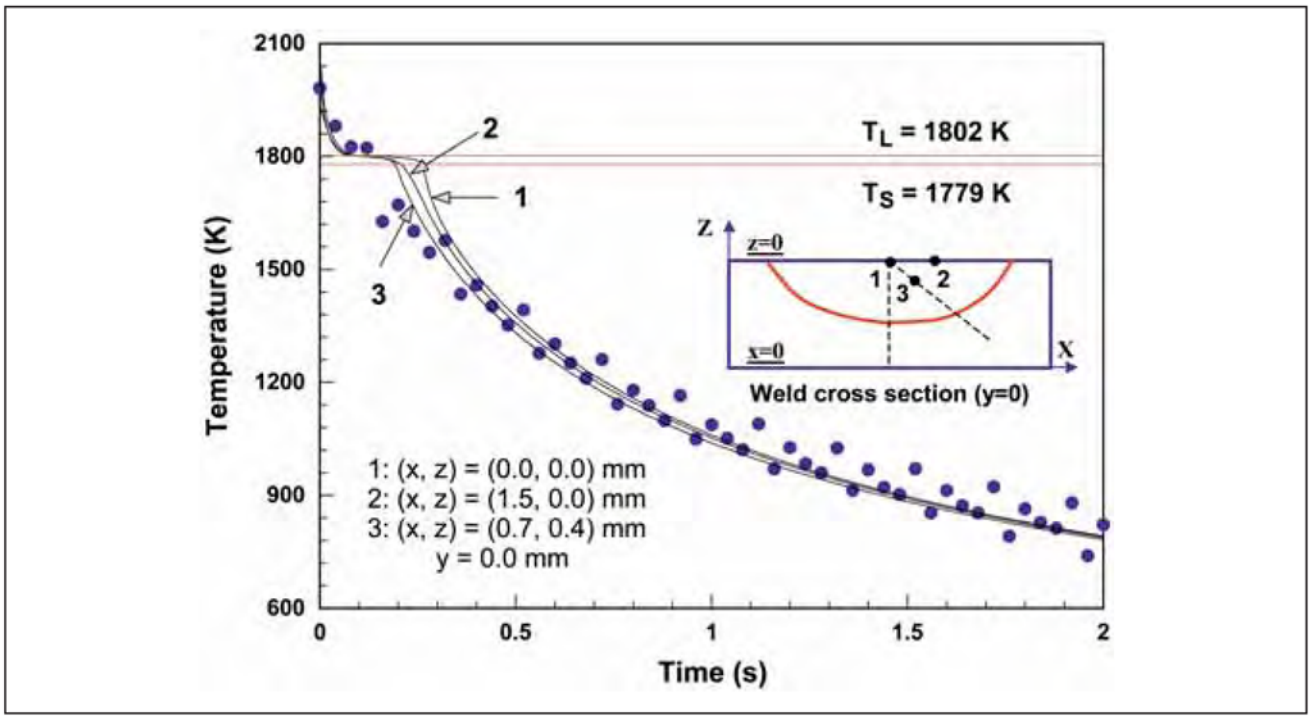

The measured cooling curve is represented by the dots.
Solid lines represent the computed cooling curves at several different locations in the weld pool, as shown in the inset figure.

Figure 4 – Comparison between the measured and calculated cooling curves

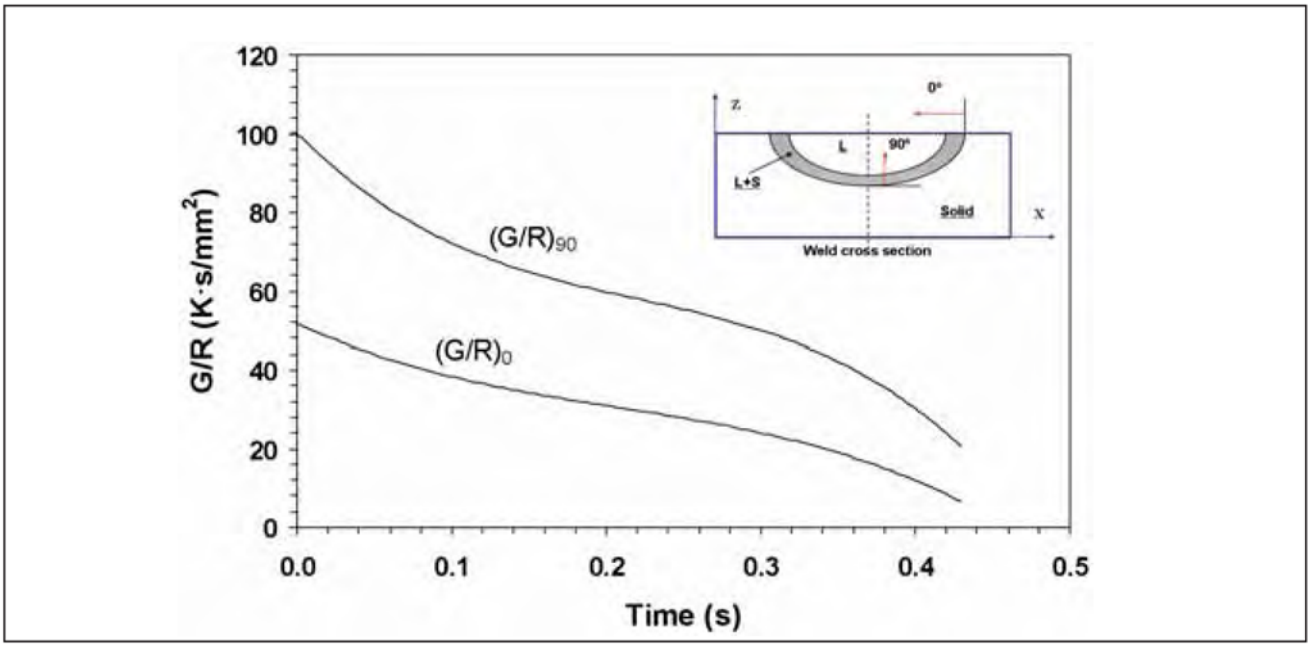

Symbols G and R represent the temperature gradients and the solidification rate, respectively.

Figure 5 – Calculated solidification parameter G/R at the 0°and 90° planes

geometrical features of the weld bead. The control of weld bead geometry is often achieved solely through trial and error procedure. This approach is inherently expensive because there are a large number of variables to be considered. Furthermore, it ignores the potential competitive technological advantage that is attainable based on fundamental understanding of welding science.

The goal of this study is to establish a framework combining experiments and modelling that serves as a basis for creating fillet welds with desired properties. A three-dimensional numerical heat transfer and fluid flow model was developed to study the temperature profile, velocity field, weld pool shape and size, and nature of the solidified weld bead geometry during GMA fillet welding. The numerical model solves the continuity, momentum conservation and energy conservation equations using a boundary fitted curvilinear coordinate system, while taking into account the weld top surface deformation as well as the additional heat from the metal droplets [6, 7].

Figure 6 shows the calculated temperature and velocity fields in a fillet weld. For clarity, only half of the workpiece is shown, since the weld is symmetric about the central longitudinal plane containing the welding direction. Figure 7 shows the calculated weld bead shape for four sets of different welding conditions. As shown in this figure, the calculated weld bead geometry agrees reasonably well with the corresponding experimental result. In particular, the shape of the weld reinforcement and the finger penetration could be satisfactorily predicted by the model. Figure 8 shows the calculated average cooling rates at two monitoring locations, i.e., fusion boundary at the top surface and the joint root, for various welding conditions. The average cooling rates at the joint root are smaller than those at the fusion boundary of the top surface because the heat is conducted away more easily at the top surface than at the central plane. The calculated cooling rates at the fusion boundary agree reasonable well with those estimated using the nomograph available in the literature [13].

The comparison of the modelling results with the experimental data reported here indicates a significant promise for understanding and controlling GMA fillet welding processes based on fundamental principles of transport phenomena.

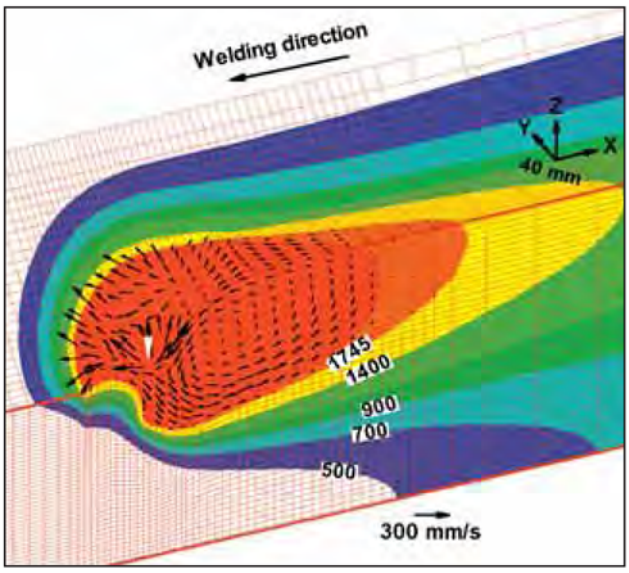

All the temperatures are given in Kelvin.
The white arrow in the middle of the weld pool indicates the location of the heat source.
The weld pool boundary is represented by the 1 745 K isothermal line.

Figure 6 – Calculated temperature and velocity fields in a fillet weld

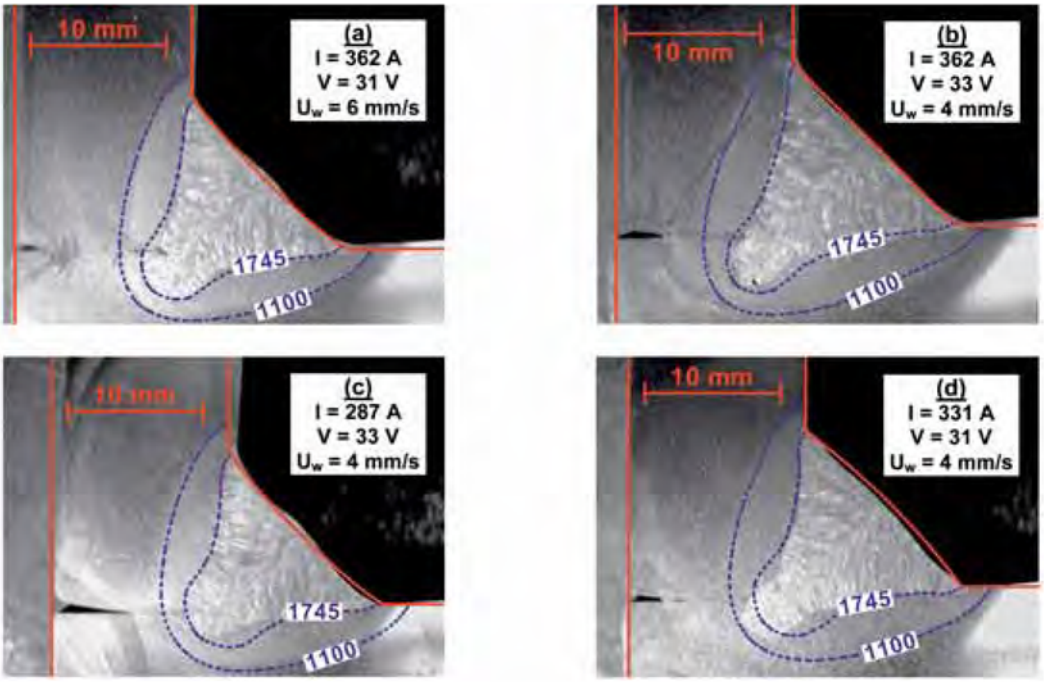

Dashed lines represent computed isotherms, and the 1 745 K solidus isotherm indicates the calculated FZ boundary. Symbols I, V and U_w represent welding current, voltage and travel speed, respectively.

Figure 7 – Calculated and experimental fillet weld geometry for different cases

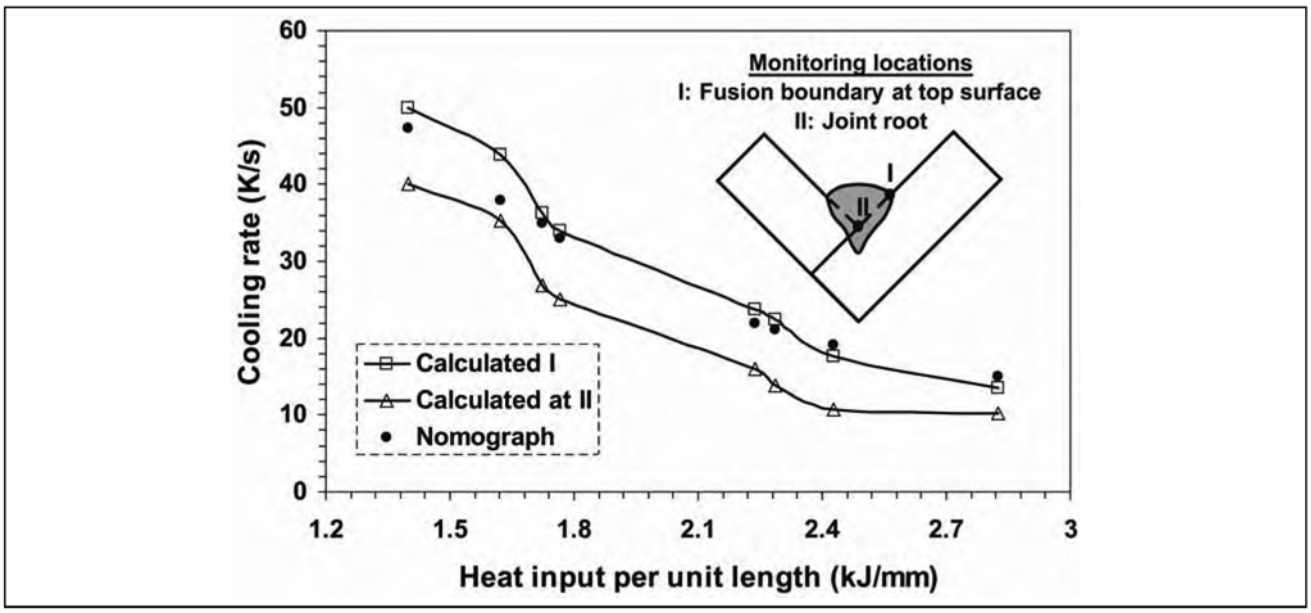

The solid dots represent the cooling rate estimated using the nomograph available in the literature [13].

Figure 8 – Calculated average cooling rate $T_{8/5}$ at two monitoring locations in the fillet weld for various welding conditions

3.3 Microstructural evolution during GTA welding of 1005 low carbon steel

The final microstructure in the weldment results from a series of transformations during both weld heating and cooling. In this work, an integrated modelling approach combining various existing models was developed to understand the microstructural evolution during GTA welding of 1005 low carbon steel. As shown in Figure 9, the ferrite to austenite transformation during heating was studied using a verified JMA analysis, the austenite grain growth was calculated using a Monte Carlo simulation, and the austenite to ferrite transformation during cooling were examined using an austenite decomposition model [9]. The integrated models were then used to predict the superheat required for the completion of the austenitization, the prior austenite grain size after the grain growth, and the volume fractions of various final microstructures in the weldment. These calculations are performed at different HAZ locations where the peak temperatures and heating and cooling rates are different, thus allowing to calculate the microstructural gradient in the HAZ.

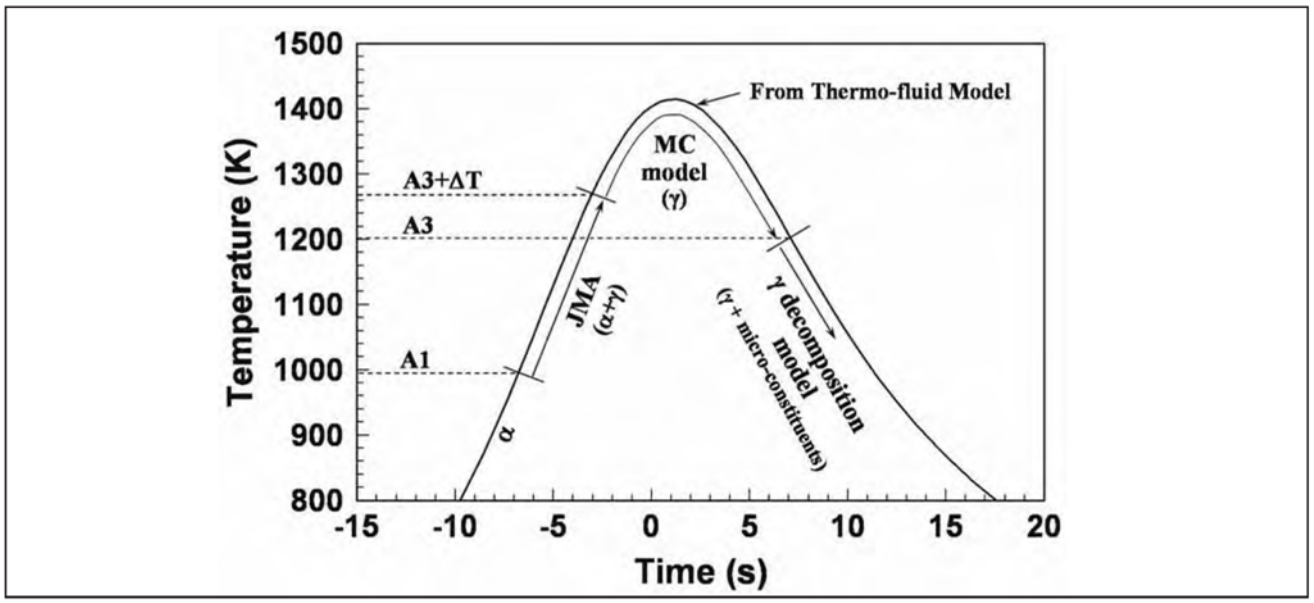

The austenitization is modelled by the verified JMA equation, the grain growth of the austenite is modelled by the MC model, and the formation of the final weld microstructure is modelled by an austenite decomposition model. The thermal cycle is calculated using the thermal-fluid model.

Figure 9 – A schematic diagram showing the main physical processes that are modelled to understand the final microstructure in the HAZ of 1005 steel during heating and cooling

Figure 10 shows the computed Continuous-Heating-Transformation (CHT) diagram using the verified JMA equation. Superimposed are the A1 (993 K) and A3 (1 204 K) temperatures for this steel. As shown in this figure, the transformation rate accelerates rapidly with temperature, and the start and finish temperatures of the transformation both increase with increasing heating rate. It is apparent that some amount of superheat is required to start and complete the phase transformation under non-isothermal conditions.

Figure 11 shows the γ grain structure at the weld top surface calculated using the MC simulation. This snapshot was taken just prior to the γ decomposition during cooling. As shown in this figure, a spatial gradient of γ grain size exists in the HAZ: larger grains are observed closer to the FZ and vice versa. Such spatial variation of grain size results from the local variation of thermal cycles and peak temperatures and can be quantified using the MC code. As shown in Figure 11, two microstructure sub-regions can be identified in the HAZ: the coarse grain region (CGR) and the fine grain region (FGR). The CGR, located near the FZ boundary, is subjected to strong thermal cycles in the HAZ. As a result, significant γ grain growth takes place in the CGR and

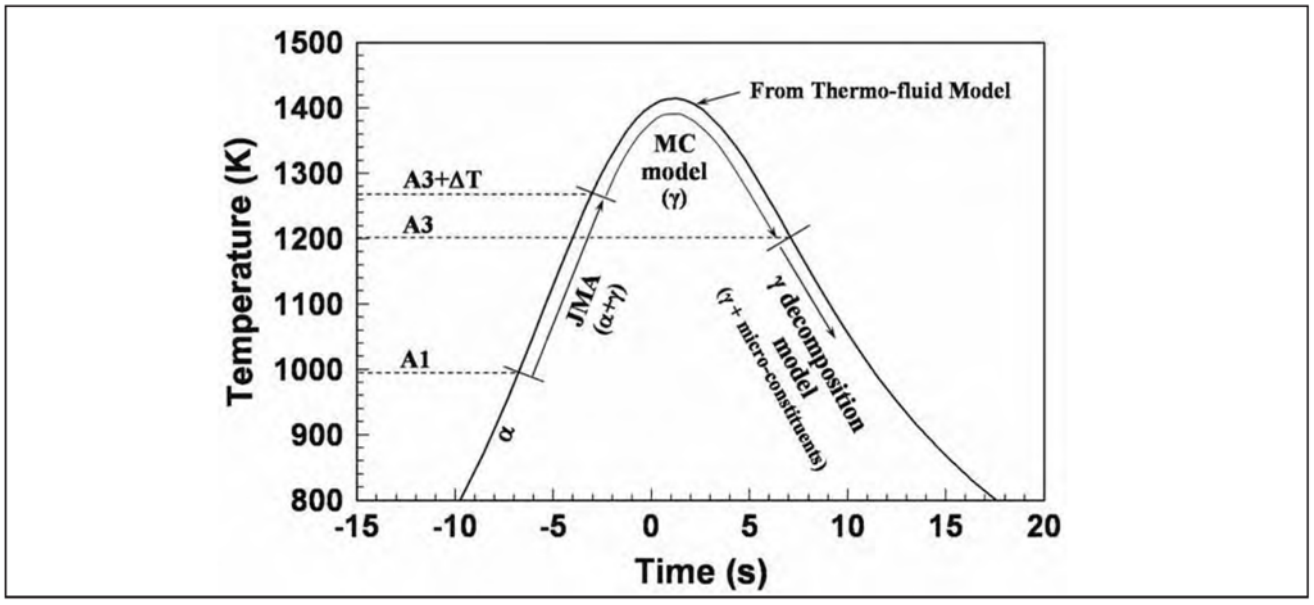

Kinetic parameters used in the calculation were determined from the x-ray diffraction data.

Figure 10 – Calculated CHT diagram for the $\alpha \rightarrow \gamma$ transformation during heating of 1005 steel

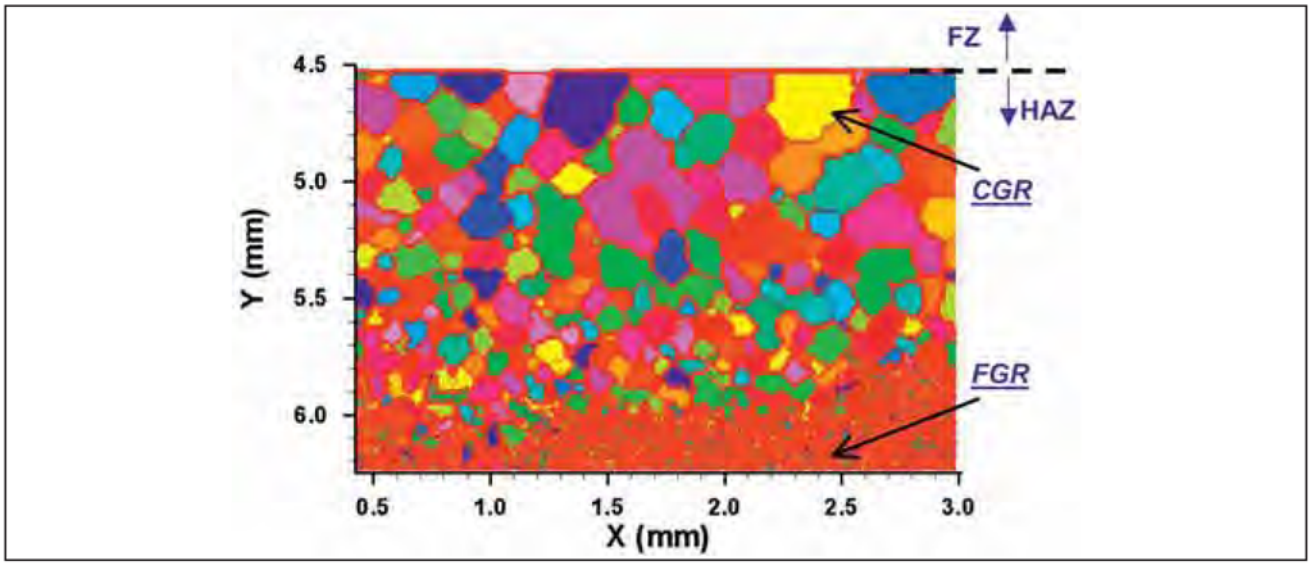

Symbols CGR and FGR represent the coarse grain region and fine grain region after the γ grain growth, respectively.

Figure 11 – Computed γ grain structure at the weld top surface prior to the austenite decomposition during cooling

large γ grains form. At a location about 1.2 mm away from the FZ boundary, the peak temperature is just slightly higher than the A3 temperature. Therefore, the transformed γ grains are "frozen" and very little grain growth occurs in the FGR.

The final microstructure at different locations in the HAZ was determined, and the results are plotted in Figures 12 a) and 12 b). These results show the spatial variation of the various microstructural constituents in the HAZ. These microconstituents are primarily allotri-

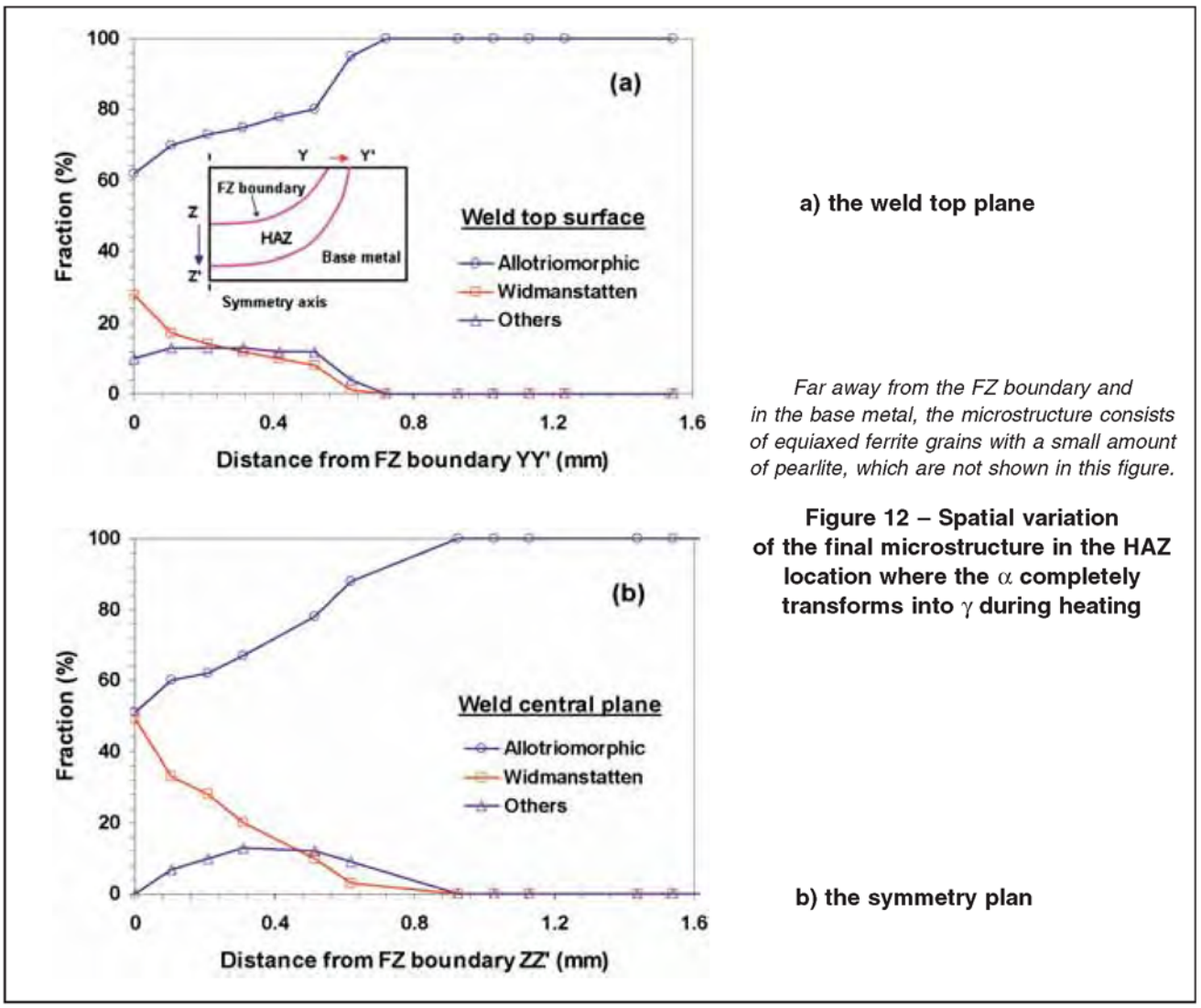

a) the weld top plane

Far away from the FZ boundary and in the base metal, the microstructure consists of equiaxed ferrite grains with a small amount of pearlite, which are not shown in this figure.

Figure 12 – Spatial variation of the final microstructure in the HAZ location where the α completely transforms into γ during heating

b) the symmetry plan

omorphic ferrite and Widmanstatten ferrite, which is consistent with the experimental observation [4]. As the distance from the FZ boundary increases, the fraction of the allotriomorphic ferrite increases, whereas that of Widmanstatten ferrite decreases. The model predictions correlated well with the available experimental data.

3.4 Phase transformation kinetics in 1045 steel and Ti-6Al-4V alloy arc welds

In this investigation, the time resolved x-ray diffraction experiments were performed during transient spot arc welding of 1045 steel [10] and Ti-6Al-4V alloy [12]. The transient heat transfer and fluid flow model was used to predict weld temperatures as a function of weld time and location. The model was validated by comparing the predicted and experimentally measured geometry of the FZ. The TRXRD results were analyzed to model the kinetics of the α-ferriterγ-austenite transformation in the 1045 steel and the α-Ti to β-Ti transformation in the Ti-6Al-4V, using the JMA model and the computed weld temperatures. The JMA kinetic analysis of the TRXRD data provided a set of kinetic parameters, allowing a quantitative means for predicting phase transformation rates under different heating conditions. Figure 13 shows the results of one of these calculations, where the transformation rates of the 1045 steel are compared to those of a 1005 steel to highlight how the carbon content and microstructure affect the transformation kinetics.

3.5 Phase transformation kinetics in 2205 DSS arc welds

The kinetics of the γ-austenite to δ-ferrite transformation during arc welding of a 2205 duplex stainless steel has been examined using a combination of experimental and modelling techniques [11]. The welding experiments involve using high energy synchrotron radiation to monitor the phases present in real-time at various locations of the weldment. The model of the $\gamma \rightarrow \delta$ transformation is based on the assumption that this transformation is driven by the diffusion of nitrogen under para-equilibrium conditions. This one-dimensional diffusion model uses a moving grid method to track the moving interfaces. The model integrates the computed thermal cycles calculated from a well-tested weld thermo-fluid model, and is capable of calculating the nitrogen diffusion across several grains with the sizes of the grains being consistent with those found in the base metal microstructure.

The diffusion model is validated by comparing the computed results with those measured experimentally using the in-situ x-ray diffraction technique, as shown in Figure 14. The effect of non-uniform starting microstructures on the transformation kinetics is simulated by considering grains of varying sizes. It is found that the transformation always completes at a later time for the non-uniform starting microstructure than for a uniform structure, as shown in Figure 15. Time-Temperature-Transformation and Continuous-Heating-Transformation diagrams are constructed using the numerical diffusion model, providing a graphical means to predict the kinetics of the $\gamma \rightarrow \delta$ transformation.

4 SUMMARY AND CONCLUSIONS

Modelling and simulation of the welding processes and materials have evolved as powerful techniques for understanding the fundamental phenomena of welding. With the advancement of computational hardware and software, it is now practical to perform integrated weld

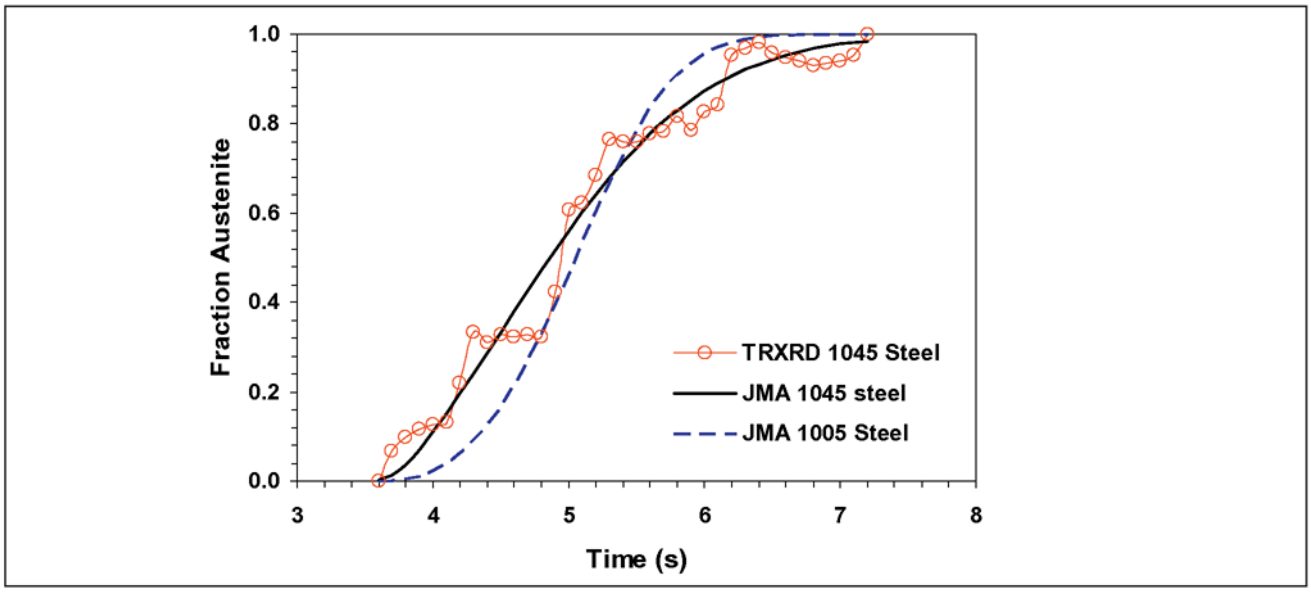

The TRXRD data for the 1045 steels are given by the solid circles and solid best-fit line, and are compared to the JMA parameters for the 1005 steel (dashed line) from the previous study.

Figure 13 – Kinetics of the ferrite to austenite transformation on weld heating

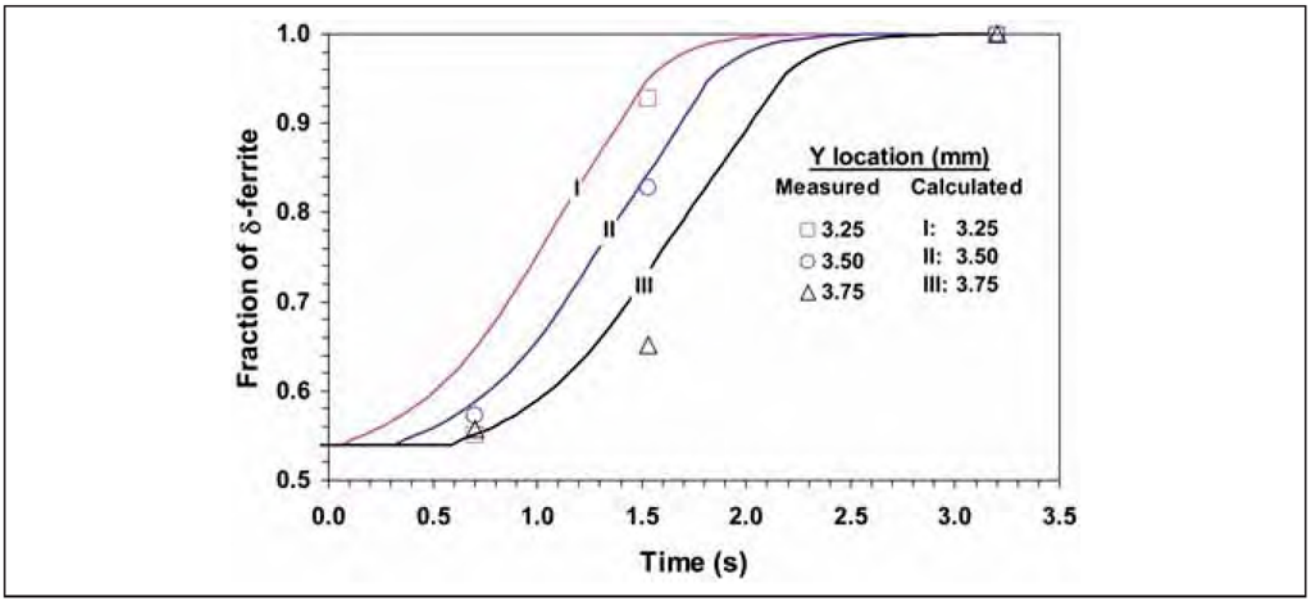

Figure 14 – Comparison of calculated and measured kinetic data at three different monitoring locations

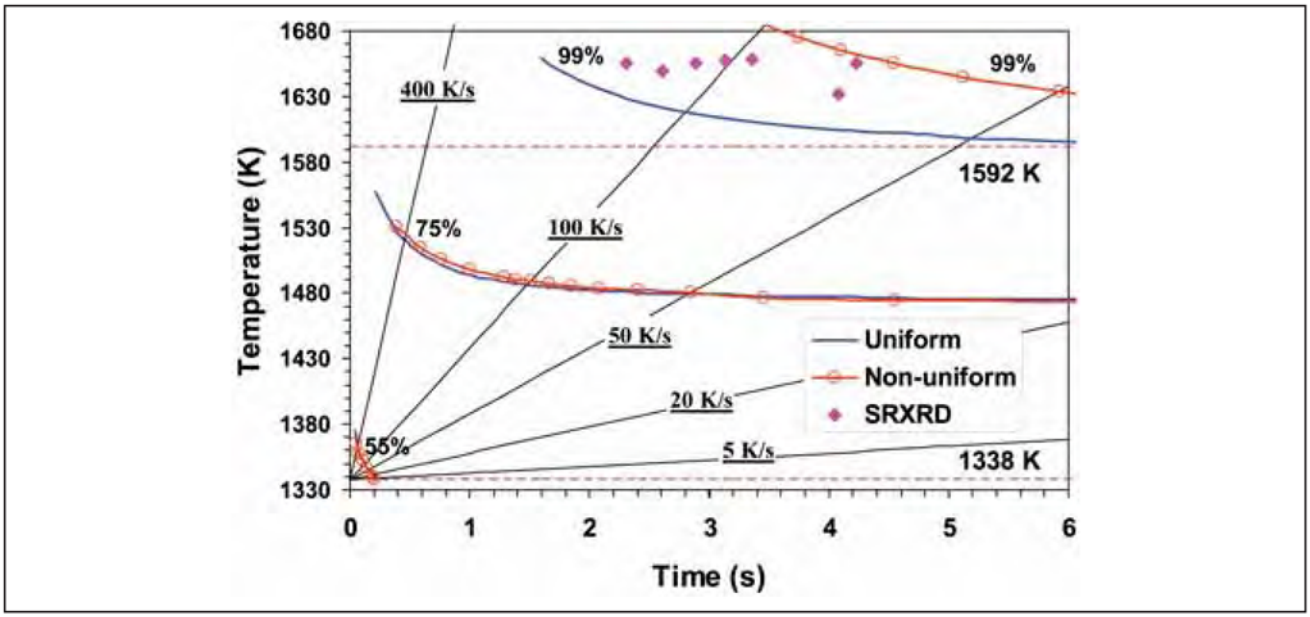

Solid diamonds represent the experimental data points at which the completion of the transformation is observed.

Figure 15 – Calculated CHT diagram for the $\gamma \rightarrow \delta$ transformation during heating of the 2205 DSS

modelling and to address realistic situations. In the present research work, a methodology synthesizing the advanced numerical tools and welding experiments has been developed and applied to study different welding scenarios. The integrated models can be run on a standard desktop personal computer (PC) and do not require a large amount of computational time. For instance, even the most computationally intensive models such as the 3-D thermal-fluid flow model and the Monte Carlo code take a few hours to do the calculations.

The integrated models developed in the present work take into account the interactions of heat, fluid flow and microstructure. The 3-D heat transfer and fluid flow model is used to understand the weld pool phenomena and provides useful insight into the physics of the weld pool. The FZ geometry, the reinforcement profile, and the thermal cycles for various welding conditions are predicted using the thermal-fluid model. Application of the computed thermal cycles and advanced phase transformation models provides a powerful tool to understand the microstructural evolution during welding. It is shown that by combing computational thermodynamics, phase transformation and transport phenomena, it is possible to predict the final weld microstructure for different materials. The model predictions are tested by well-designed experimental work based on real-time x-ray diffraction technique.

Systematic tailoring of weld attributes based on scientific principles remains an important goal to fabricate reliable welds. The present research work shows that this need can be fulfilled utilizing multidisciplinary models representing the complex physical processes of welding. This work demonstrates that the application of

numerical transport phenomena can significantly add to the quantitative knowledge base in welding and help the welding community in solving practical problems. Apart from serving as a basis for understanding the existing welding processes and materials, the multidisciplinary modelling framework developed here will meet the need for newly developed welding processes and welding of a new class of advanced engineering materials.

The future directions of the integrated modelling framework include
(1) integrating the mechanical models,
(2) accounting for complex interactions of different physical processes, and
(3) automating modelling process.

It is hoped that such integrated model combines heat transfer, fluid flow, microstructure evolution, and stresses and distortion will enable us to design better welds utilizing advanced simulation.

ACKNOWLEDGEMENTS

The PennState portion of the work was supported by a grant from the U.S. Department of Energy, Office of Basic Energy Sciences, Division of Materials Sciences, under grant number DE-FGO2-01ER45900. The LLNL portion of this research was performed under the auspices of the U.S. Department of Energy, Lawrence Livermore National Laboratory, under Contract No. W-7405-ENG-48. Dr. Zhang gratefully acknowledges the award of a Fellowship from the American Welding Society (AWS).

REFERENCES

[1] David S.A., DebRoy T.: Science, 1992, 257, 497.

[2] DebRoy T., David S.A.: Rev. Mod. Phys., 1995, 67, 85.

[3] Zhang W.: Probing heat transfer fluid flow and microstructural evolution during fusion welding of alloys, Ph.D. Dissertation, The Pennsylvania State University, May 2004.

[4] Zhang W., Elmer J.W., DebRoy T.: Mater. Sci. Eng. A, 2002, 333, 320.

[5] Zhang W., Roy G.G., Elmer J.W., DebRoy T.: J. Appl. Phys., 2003, 93, 3022.

[6] Zhang W., Kim C-H., DebRoy T.: J. Appl. Phy., 2004, 95, 5210.

[7] Zhang W., Kim C-H., DebRoy T.: J. Appl. Phy., 2004, 95, 5220.

[8] Elmer J.W., Palmer T.A., Zhang W., Wood B., DebRoy T.: Acta Mater., 2003, 51, 3333.

[9] Zhang W., Elmer J.W., DebRoy T.: Sci. Technol. Weld. Joining, 2005, 10, 574.

[10] Elmer J.W., Palmer T.A., Babu S.S., Zhang W., DebRoy T.: Weld. J., 2004, 83, 244s.

[11] Zhang W., DebRoy T., Palmer T.A., Elmer J.W.: Acta Mater., 2005, 53, 4441.

[12] Elmer J.W., Palmer T.A., Babu S.S., Zhang W., DebRoy T.: J. Appl. Phys., 2004, 95, 8327.

[13] Masubuchi K.: Analysis of Welded Structures, Pergamon, Oxford, 1980.